

M-ary Bayes Estimator Selection for QuikSCAT Simultaneous Wind and Rain Retrieval

Michael P. Owen and David G. Long, *Fellow, IEEE*

Abstract—While originally designed only for wind measurement, the QuikSCAT scatterometer is capable of making wind and rain estimates over the ocean. Three separate estimators are used, a wind-only estimator, a rain-only estimator, and a simultaneous wind–rain estimator. No one of the estimators is suitable under all wind and rain conditions. We therefore propose a Bayesian estimator selection technique whereby the appropriate estimator can be selected from the estimates themselves. This paper introduces the Bayes estimator selection technique and discusses its application to QuikSCAT wind and rain estimation for conventional (25-km) resolution products. Results indicate that using Bayes estimator selection can improve both the bias and mean-squared error of wind estimates in both raining and nonraining conditions, as well as provide an improved rain flag.

Index Terms—Bayes estimation, QuikSCAT, resolution enhancement, scatterometry, simultaneous wind/rain retrieval, wind retrieval.

I. INTRODUCTION

WIND and rain estimation over the ocean is possible using data provided by the QuikSCAT scatterometer. The QuikSCAT scatterometer is designed to measure the radar cross section or backscatter of the ocean. A model function is used to infer the most likely wind vector to have produced the observed measurements [1]–[3]. Unfortunately, rain adversely affects wind estimation. It is estimated that rain affects 4% to 10% of all QuikSCAT observations. Recently, rain retrieval from QuikSCAT measurements has been demonstrated [4]–[6]. To account for rain, three slightly different estimation techniques may be employed: wind-only (WO), simultaneous wind–rain (SWR), and rain-only (RO) estimators. The performance of each estimator is dependent on the underlying wind–rain conditions. Each estimation technique is best under certain backscatter conditions, and no single technique is suitable for all conditions. By adaptively selecting the estimator most appropriate to the true conditions, the overall wind and rain measurement performance can surpass that of any individual estimator.

In this paper, we introduce Bayes estimator selection, a technique whereby a single “best” estimator is selected for each wind–rain condition. We then apply the technique to QuikSCAT

wind and rain estimation. Section II discusses and motivates the multiple estimator problem, Section III gives relevant background information about the QuikSCAT scatterometer, Section IV introduces Bayes estimator selection in a general sense, Section V discusses the application of Bayes estimator selection to QuikSCAT wind and rain estimation, Section VI gives an overview of Bayes estimator selection results, and Section VII concludes.

II. PROBLEM FORMULATION

The QuikSCAT scatterometer was designed for the express purpose of wind estimation over the ocean. The traditional wind estimation process that retrieves only the near-surface wind is what we term the WO estimation in the following discussion [7]. QuikSCAT WO estimates have good performance in most wind conditions; however, the estimates can be degraded by rain. Rain contamination has been traditionally dealt with using one of several rain flagging techniques to identify rain contaminated winds (see, for example, [8]). Rain-flagged wind estimates have typically been discarded.

SWR estimation has been proposed as an alternative solution to rain flagging of rain-contaminated winds [4]. SWR estimation improves WO estimation by adjusting the WO model to account for both wind and rain effects on the radar backscatter [9], [10]. Replacing the wind model with the joint wind–rain model and estimating both the wind and the rain is what we term the SWR estimation [4], [10]. However, for nonraining cases, SWR estimation can degrade the performance compared to WO estimation. This is due, in large part, to the fact that noise in the backscatter measurements can sometimes cause nonraining observations to resemble raining cases, resulting in cases where SWR estimation has a nonzero rain estimate yet no rain is occurring. To minimize this SWR sensitivity to nonrain observations, SWR estimation in this paper is constrained to ignore solutions with zero rain rates and zero wind speeds. This makes SWR estimation distinct from WO estimation and RO estimation since they cannot retrieve the same solutions.

For rain events with high rain rates and rain-dominated backscatter [11], the wind and rain estimates for SWR estimation may be degraded. Essentially, for certain wind speed and rain rate combinations, the wind–rain model breaks down due to high rain-induced attenuation and the consequent loss of wind signal, causing the SWR estimates to be inaccurate. For these rare high rain cases, wind cannot be estimated, although RO estimation can provide accurate results [6].

In RO estimation [6], the wind model is discarded entirely, and only the rain model is used; hence, only a rain estimate

Manuscript received August 4, 2010; revised March 3, 2011; accepted April 11, 2011. Date of publication June 9, 2011; date of current version October 28, 2011.

The authors are with the Microwave Earth Remote Sensing Laboratory, Brigham Young University, Provo, UT 84602 USA (e-mail: owen@mers.byu.edu; long@ee.byu.edu).

Color versions of one or more of the figures in this paper are available online at <http://ieeexplore.ieee.org>.

Digital Object Identifier 10.1109/TGRS.2011.2143721

is produced. RO estimation makes the assumption that wind has essentially no effect on the radar backscatter, which can occur under high rain conditions. For these cases, the rain accuracy is much improved by this assumption versus using SWR estimation.

In summary, there are three different estimation techniques which are appropriate under different conditions. Each performs well under appropriate conditions; however, if the estimator is used outside of the intended conditions, the estimator performance is degraded. There is therefore no single estimator that is suitable for all conditions. Instead of choosing one estimator and using it under all conditions, we propose a Bayesian estimator selection method whereby the three estimators are compared and a single estimate is chosen from the various estimates from the set of estimators.

III. BACKGROUND

Before discussing estimator selection, an overview of the QuikSCAT scatterometer and wind and rain estimation is prudent. QuikSCAT measures the normalized radar backscatter σ^o of the Earth's surface at the Ku-band. Measurements are made using a rotating dual-polarization antenna which forms a 1800-km-wide swath on the surface.

A. Wind and Rain Estimators

For a wind vector $\mathbf{w} = [s, d]$ with wind speed s and direction d , rain rate r , and a wind-rain vector $\vartheta = [w, r]$, the backscatter σ^o can be modeled phenomenologically as [4], [5], [9]

$$\sigma^o = \alpha_r \sigma_w + \sigma_e \quad (1)$$

where σ_w is the backscatter from the ocean surface due to wind, $\alpha_r(r)$ is the attenuation factor of the ocean wind backscatter due to atmospheric rain, and $\sigma_e(r)$ is the effective rain backscatter from both the rain volume scattering and attenuated surface scattering due to additional splashes and waves. For wind and rain retrieval, the phenomenological model is calculated for each measurement using

$$\mathcal{M}_r(\vartheta, \chi, \psi, p) = \mathcal{M}(\mathbf{w}, \chi, \psi, p) \alpha_r(r, p) + \sigma_e(r, p) \quad (2)$$

where $\mathcal{M}_r(\vartheta, \chi, \psi, p)$ is the combined wind and rain model. Here, $\mathcal{M}(\mathbf{w}, \chi, p)$ is the wind geophysical model function (GMF) which gives the expected wind backscatter for a wind vector \mathbf{w} given the antenna azimuth angle χ , incidence angle ψ , and polarization p . The rain model terms $\alpha_r(r, p)$ and $\sigma_e(r, p)$ correspond to the phenomenological model of (1) with subscripts to indicate that they are functions of rain rate r and polarization p .

In this paper, the wind backscatter GMF $\mathcal{M}(\mathbf{w}, \chi, p)$ refers to the standard QuikSCAT QMOD4 GMF [12]. The QMOD4 GMF has been demonstrated to be an appropriate model for Ku-band backscatter for QuikSCAT observation geometry; however, for hurricane-force winds (> 30 m/s), the GMF has limited validity due to backscatter saturation. Since an assessment of the QuikSCAT GMF is beyond the scope of this

paper, we acknowledge the GMF limitations and focus the results portion of this paper on conditions in which the National Centers for Environmental Prediction (NCEP) model winds are low to moderate (< 20 m/s).

The rain attenuation and backscatter model parameters are specified in [4] and are assumed to be independent of wind velocity and antenna azimuth angle. Because the terms χ , ψ , and p are determined by the measurement geometry, we simplify the notation in the following by dropping them and leaving only the wind and rain dependence.

Wind and rain estimation is performed using the backscatter model and the QuikSCAT backscatter measurement noise model. The measurement model assumes a Gaussian noise distribution with mean $\mathcal{M}_r(\vartheta)$ and can be written as

$$f(\sigma_i^o | \vartheta) = \frac{1}{\sqrt{2\pi\zeta}} \exp\left(-\frac{1}{2\zeta^2} (\sigma_i^o - \mathcal{M}_r(\vartheta))^2\right) \quad (3)$$

where σ_i^o is the backscatter observation for the i th measurement, ϑ is the true wind-rain vector, $\mathcal{M}_r(\vartheta)$ is the model backscatter as a function of the true wind-rain vector, and ζ^2 is the model variance. The model variance can be written as [4]

$$\zeta^2 = (1 + K_{pc}^2) [\alpha_r(r)^2 \mathcal{M}(\mathbf{w})^2 K_{pm}^2 + \sigma_e(r)^2 K_{pe}^2] + \mathcal{M}_r(\vartheta)^2 K_{pc}^2 \quad (4)$$

where K_{pc} is the normalized standard deviation of the communication noise, K_{pm} is the normalized standard deviation of the wind backscatter model, and K_{pe} is the normalized standard deviation of the effective rain backscatter model. The communication noise term for QuikSCAT is modeled as

$$K_{pc} = \sqrt{\alpha + \frac{\beta}{\mathcal{M}_r(\vartheta)} + \frac{\gamma}{\mathcal{M}_r(\vartheta)^2}} \quad (5)$$

where the parameters α , β , and γ are geometry and resolution dependent [13].

Maximum likelihood estimates for wind and rain can be formed using the log-likelihood function of the measurement model [7]. The maximum likelihood estimate is the wind-rain vector which maximizes the likelihood function and can be written as

$$\hat{\vartheta} = \arg \max_{\vartheta} \sum_i \left(-\log(\sqrt{2\pi\zeta}) - \frac{1}{2\zeta^2} (\sigma_i^o - \mathcal{M}_r(\vartheta))^2 \right) \quad (6)$$

where the summation is over the vector of backscatter observations. The WO, RO, and SWR estimators are each calculated similarly and differ only by the models used for the mean and variance in (3). For WO estimation, $\mathcal{M}_r(\vartheta) = \mathcal{M}(\mathbf{w})$. For RO, $\mathcal{M}_r(\vartheta) = \sigma_e(r)$. Moreover, for SWR, $\mathcal{M}_r(\vartheta)$ is used as defined in (2). The variance model for each estimator also changes accordingly, see Table I.

The simple phenomenological model in (1) can be used to motivate each estimation technique. When rain is not present, i.e., $\alpha_r = 1$ and $\sigma_e = 0$, σ^o is only a function of σ_w , and WO estimation produces the best estimate. Similarly, when σ^o is dominated by σ_e and α_r , i.e., $\alpha_r \ll 1$, RO estimation is appropriate. When the wind and rain signals are of similar magnitude,

estimating them jointly using SWR estimation produces the best performance. In essence, depending on the true conditions, one of the estimators produces a better estimate of wind, wind and rain, or rain.

B. Estimator Bounds

Before discussing estimator selection, it is important to quantify the limitations of each of the estimators. One method to quantify estimator performance is to evaluate the theoretic limitations of each estimator using the Cramer–Rao bound (CRB). As discussed previously, the introduction of contamination due to unmodeled phenomena causes a bias in the estimates. Thus, we must adopt the biased form for the CRB. The CRB for WO, SWR, and RO retrieval [5], [14] can be written as

$$E \left[(\hat{\vartheta} - \vartheta)(\hat{\vartheta} - \vartheta)^T \right] \geq \frac{\partial E[\hat{\vartheta}]}{\partial \vartheta} J^{-1}(\vartheta) \left[\frac{\partial E[\hat{\vartheta}]}{\partial \vartheta} \right]^T \quad (7)$$

where the elements J_{ij} of the Fisher information matrix J are

$$J_{ij}(\vartheta) = \sum_{k=1}^N \frac{\partial \mathcal{M}_{rk}}{\partial w_i} \frac{1}{\zeta_k^2} \frac{\partial \mathcal{M}_{rk}}{\partial w_j} + \frac{\partial \zeta_k^2}{\partial w_i} \frac{1}{2\zeta_k^4} \frac{\partial \zeta_k^2}{\partial w_j}. \quad (8)$$

Here, the Fisher information is represented for wind and rain estimation. The Fisher information for WO estimation is a special case of the wind and rain information where the rain rate is 0. Note that for WO retrieval, J is a 2×2 matrix since $\hat{\vartheta} = \hat{\mathbf{w}}$, whereas for SWR retrieval, J is a 3×3 matrix since $\hat{\vartheta} = (\hat{\mathbf{w}}, \hat{r})$.

The biased CRB can be calculated similarly for rain-contaminated WO retrieval by adjusting the Fisher-information matrix for the rain contamination

$$J_{ij}(\vartheta) = \sum_{k=1}^N \frac{\partial \mathcal{M}_k}{\partial w_i} \frac{\alpha_r^2}{\zeta_k^2} \frac{\partial \mathcal{M}_k}{\partial w_j} + \frac{\partial \zeta_k^2}{\partial w_i} \frac{1}{2\zeta_k^4} \frac{\partial \zeta_k^2}{\partial w_j}. \quad (9)$$

Like the WO Fisher information, the rain-contaminated Fisher information is a 2×2 matrix since $\hat{\vartheta} = \hat{\mathbf{w}}$. However, for rain contamination, the Fisher information is also dependent on r , so we can write $J_{ij}(\mathbf{w}, r)$.

Similarly, the biased CRB can be calculated for wind-contaminated RO retrieval using

$$J(\mathbf{w}, r) = \sum_{k=1}^N \left(\mathcal{M}_k \frac{\partial \alpha_r}{\partial r} + \frac{\partial \sigma_e}{\partial r} \right)^2 \frac{1}{\zeta_k^2} + \frac{\partial \zeta_k^2}{\partial r} \frac{1}{2\zeta_k^4} \frac{\partial \zeta_k^2}{\partial r}. \quad (10)$$

Here, we have explicitly separated the wind vector \mathbf{w} and rain rate r in the notation to make it clear that the derivatives are with respect to the rain rate and that the wind contamination is a function of the wind vector. Also note that the RO CRB is a scalar value that is only valid for the rain rate estimate.

The CRBs for 25-km-resolution wind speed and rain estimators are shown in Fig. 1. To jointly compare the bounds on wind and rain estimation accuracy, we form an *overall* CRB by taking a linear combination of the wind speed and rain rate bounds for each estimator where the weighting coefficients are selected to reflect the relative importance that we place on

wind or rain accuracy. Comparing the estimation bounds for the several estimators makes it apparent that there are regions in the wind and rain space where a particular estimator outperforms the others. For example, Fig. 1 indicates that ignoring rain under low rain conditions, as the WO estimator does, results in wind estimates with a lower overall mean-squared error. Similarly, when the wind speed is low and the rain rate is moderate to high, the RO estimator has lower mean-squared error than the SWR estimator. Fig. 2 summarizes Fig. 1 by indicating the estimator which has the minimum overall CRB for each wind and rain vector. Finally, note that the SWR estimates often have a larger bound than either the WO or the RO estimators. This observation is central to the remainder of this paper and prompts the following question: If one estimator does not always have the lowest overall CRB, how can the estimator with the lowest overall CRB be selected consistently?

IV. M-ARY BAYES ESTIMATOR SELECTION

M-ary Bayes estimator selection is a modification of the Bayes decision theory. It operates on the estimates produced by M different estimators. In M-ary Bayes estimator selection, we attempt to select one “best” estimate from among M candidate estimates. To introduce the method, we follow the discussion and notation for the Bayes decision theory outlined in [15].

The object of the Bayes decision technique is to choose a decision rule that minimizes the Bayes risk function given a realization \mathbf{x} of the observation random variable \mathbf{X} . For estimator selection, the “observations” are the various estimates, and the parameter θ corresponds to true conditions. Although in the previous section, ϑ referred specifically to a wind vector, here, we generalize and treat ϑ as a realization of the random variable θ which represents the true conditions. The observations, or estimates, are realizations \mathbf{x}_i of the random variable \mathbf{X} . The decision rule $\phi_j(\mathbf{x}_i)$ is the rule for choosing estimate \mathbf{x}_j as the best based on the observation of the estimate being tested \mathbf{x}_i .

The loss function $L[\vartheta, \phi_j(\mathbf{x}_i)]$ represents the loss resulting from choosing the estimate \mathbf{x}_j when ϑ is the true condition. For our application, we choose the loss function

$$L[\vartheta, \phi_j(\mathbf{x}_i)] = C(\vartheta, \mathbf{x}_j) (\kappa_j \delta_{ij} + \tau_j (1 - \delta_{ij})) \quad (11)$$

where $C(\vartheta, \mathbf{x}_j)$ is a cost function, i.e., the cost of selecting \mathbf{x}_j using the decision rule ϕ_j when ϑ is the true condition. Because the decision rule ϕ_j selects estimate \mathbf{x}_j regardless of the estimate being tested, the cost of a decision rule ϕ_j only depends on the estimate \mathbf{x}_j . The term $(\kappa_j \delta_{ij} + \tau_j (1 - \delta_{ij}))$, where κ_j and τ_j are scalar weighting factors and δ_{ij} is a Kronecker delta function, allows the loss function to vary depending on which estimate is being tested. For example, when $\kappa_j = 1$ and $\tau_j = 0$, the loss function for the decision rule is zero when testing other estimators. When $\kappa_j = 0$ and $\tau_j = 1$, the loss is zero when testing the selected estimator but nonzero when other estimators are tested. The κ_j and τ_j terms thus allow for tuning the algorithm to meet the desired specifications. The weighting coefficients κ_j and τ_j must be related; however, we postpone the definition of their relationship until later.

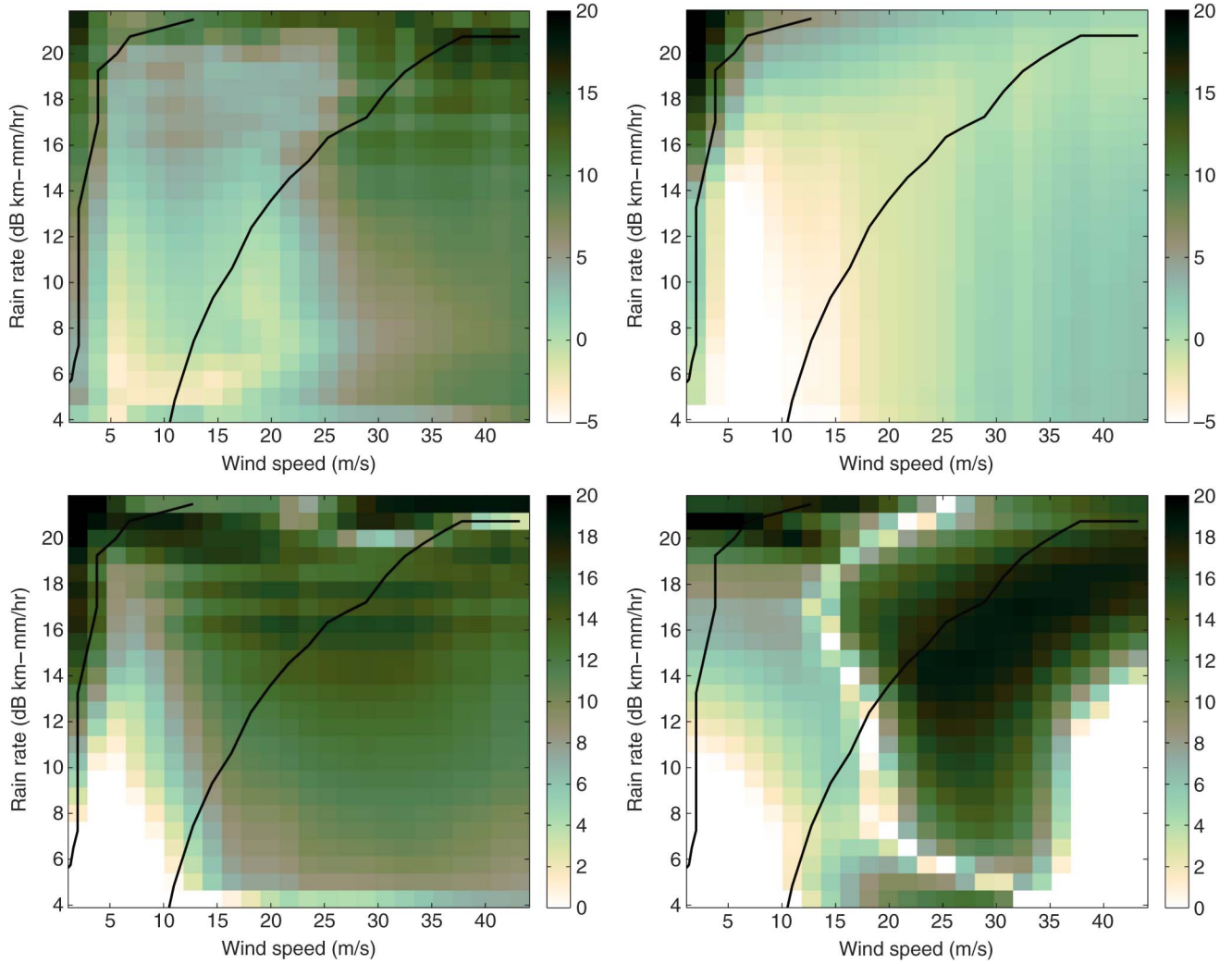


Fig. 1. CRBs in decibels on wind speed and rain rate for the various estimators. (Upper left) CRB for SWR wind speed. (Upper right) CRB for WO wind speed. (Lower left) CRB for SWR rain rate. (Lower right) CRB for RO rain rate. Note that each estimator has a region in wind speed and rain rate where the CRB is lower than the others. The bounds shown are for a single wind direction (53°) and cross-track location (cell 13) which have performance that is representative of all other wind directions. Estimator characteristics have some slight changes as a function of cross-track location due to the changing observation geometry but are generally similar. For reference, the smoothed boundaries from Fig. 2 are included in each image.

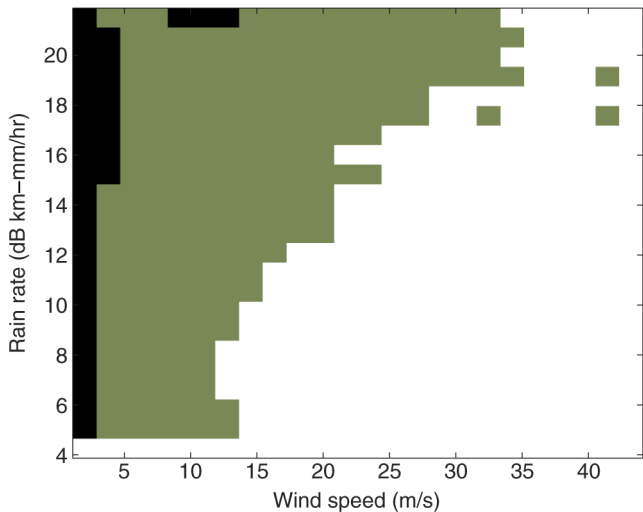


Fig. 2. Estimators with total minimum normalized CRB as a function of wind speed and rain rate: (white) WO, (gray) SWR, and (black) RO. As expected, the WO estimator is best for low rain rates and substantial wind speed, the SWR estimator is best for comparable wind speed and rain rate, and the RO estimator is best when the wind is low and rain is substantial.

A. Bayes Risk

Using the established notation, the risk function $R(\vartheta, \phi_j)$ is defined to be the expected loss of using decision rule ϕ_j under the true conditions ϑ

$$\begin{aligned}
 R(\vartheta, \phi_j) &= E_{\mathbf{X}} (L[\vartheta, \phi_j(\mathbf{x}_i)]) \\
 &= \sum_{i=0}^M L[\vartheta, \phi_j(\mathbf{x}_i)] f_{\mathbf{X}|\vartheta}(\mathbf{x}_i|\vartheta) \\
 &= \sum_{i=0}^M C(\vartheta, \mathbf{x}_j)(\kappa_j \delta_{ij} + \tau_j (1 - \delta_{ij})) f_{\mathbf{X}|\vartheta}(\mathbf{x}_i|\vartheta) \\
 &= C(\vartheta, \mathbf{x}_j) (\tau_j (1 - f_{\mathbf{X}|\vartheta}(\mathbf{x}_j|\vartheta)) + \kappa_j f_{\mathbf{X}|\vartheta}(\mathbf{x}_j|\vartheta)) \\
 &= C(\vartheta, \mathbf{x}_j) (\tau_j f_{\mathbf{X}|\vartheta}(\sim \mathbf{x}_j|\vartheta) + \kappa_j f_{\mathbf{X}|\vartheta}(\mathbf{x}_j|\vartheta)) \quad (12)
 \end{aligned}$$

where $E_{\mathbf{X}}$ denotes the expectation operator over \mathbf{X} and we define the density $f_{\mathbf{X}|\vartheta}(\sim \mathbf{x}_j|\vartheta) = 1 - f_{\mathbf{X}|\vartheta}(\mathbf{x}_j|\vartheta)$.

The Bayes risk $r(F_\theta, \phi_j)$ is the posterior expected risk function

$$\begin{aligned} r(F_\theta, \phi_j) &= E_\theta (R(\vartheta, \phi_j)) \\ &= \int_\theta R(\vartheta, \phi_j) f_\theta(\vartheta) d\vartheta \\ &= \int_\theta C(\vartheta, \mathbf{x}_j) (\tau_j f_{\mathbf{x}_j|\theta}(\sim \mathbf{x}_j|\vartheta) + \kappa_j f_{\mathbf{x}_j|\theta}(\mathbf{x}_j|\vartheta)) \\ &\quad \times f_\theta(\vartheta) d\vartheta. \end{aligned} \quad (13)$$

Using the Bayes rule, the Bayes risk can be rewritten in terms of expectations resulting in

$$r(F_\theta, \phi_j) = \tau_j E_{\theta|\sim \mathbf{X}} [C(\vartheta, \mathbf{x}_j)] f(\sim \mathbf{x}_j) + \kappa_j E_{\theta|\mathbf{X}} [C(\vartheta, \mathbf{x}_j)] f(\mathbf{x}_j) \quad (14)$$

where $E_{\theta|\sim \mathbf{X}}[C(\vartheta, \mathbf{x}_j)]$ represents the expected loss associated with the estimate given that it is not the best and $E_{\theta|\mathbf{X}}[C(\vartheta, \mathbf{x}_j)]$ is the expected loss associated with the estimate x_j given that it is the best. This formulation gives insight into the role of τ_j and κ_j . We can interpret the Bayes risk for a given estimator rule as a weighted linear combination of the expected loss given that the estimator is the best and the expected loss given that the estimator is not the best.

To compare the Bayes risk for the different estimators, it is important that the risks be comparable. A major impediment to this utility are the weighting factors $f(\mathbf{x}_j)$ and $f(\sim \mathbf{x}_j)$. If an estimator is superior more often than the others, then the Bayes risk for that estimator is more strongly weighted. This effect is ameliorated by defining τ_j and κ_j such that

$$\tau_j = \frac{\tau}{f(\sim \mathbf{x}_j)} \quad (15)$$

$$\kappa_j = \frac{\kappa}{f(\mathbf{x}_j)} \quad (16)$$

where τ and κ are weighting factors that apply to all estimates.

The Bayes risk can then be written

$$r(F_\theta, \phi_j) = \tau E_{\theta|\sim \mathbf{X}} [C(\vartheta, \mathbf{x}_j)] + \kappa E_{\theta|\mathbf{X}} [C(\vartheta, \mathbf{x}_j)]. \quad (17)$$

Thus, the Bayes risk for a given estimator is a linear combination of the conditional expected costs. Without loss of generality, we can add the constraint $\tau + \kappa = 1$. This additional constraint defines the Bayes risk for an estimator as a convex combination of the expected costs.

The Bayes decision rule for estimator selection is the rule that minimizes the Bayes risk. Such a rule can be written as

$$k = \arg \min_j r(F_\theta, \phi_j) \quad (18)$$

$$= \arg \min_j \tau E_{\theta|\sim \mathbf{X}} [C(\vartheta, \mathbf{x}_j)] + \kappa E_{\theta|\mathbf{X}} [C(\vartheta, \mathbf{x}_j)] \quad (19)$$

where k indicates that estimator \mathbf{x}_k is the best.

Although, notationally, M-ary Bayes estimator selection is similar to traditional Bayes decisions, the M-ary Bayes decision concept is distinct. In the Bayes decision theory, decisions are based on realizations of a random variable. Bayes estimator selection makes a distinction from Bayes decisions because the random variable realizations are parameter estimates made from other observations. With this generalized perspective, the

estimates can be produced with any estimation method, such as maximum likelihood, maximum *a posteriori*, or any other function of the measurements. Additionally, Bayes estimator selection places no constraints on the dimensionality of the estimators, which can be different for each. The lack of constraint on the dimensionality makes this technique particularly useful to QuikSCAT wind and rain estimation.

B. Cost Function

With the basic framework of Bayes estimator selection established, the structure can be adapted to meet particular performance criteria for the estimators \mathbf{x}_i . The desired performance criteria are specified by means of the cost function $C(\vartheta, \mathbf{x}_i)$, which reflects the goal of choosing the best estimator given the observations.

Although there are many cost functions which could be appropriate for a particular problem, for this case, we consider the squared error of the observed estimator \mathbf{x}_i given ϑ , the true conditions. The cost function $C(\vartheta, \mathbf{x}_i)$ is written as

$$C(\vartheta, \mathbf{x}_i) = (\vartheta - \hat{\mathbf{x}}_i)^2 \quad (20)$$

where

$$(\vartheta - \hat{\mathbf{x}}_i)^2 \triangleq (\vartheta - \hat{\mathbf{x}}_i)^T N (\vartheta - \hat{\mathbf{x}}_i) \quad (21)$$

is a shorthand notation for the total normalized squared error. In this case, the matrix N is a diagonal matrix with normalization coefficients to ensure the vector components are comparable. Inserting this cost function into (17) results in

$$r(F_\theta, \phi_j) = \tau E_{\theta|\sim \mathbf{X}} [(\vartheta - \hat{\mathbf{x}}_j)^2] + \kappa E_{\theta|\mathbf{X}} [(\vartheta - \hat{\mathbf{x}}_j)^2]. \quad (22)$$

This notation helps clarify the meaning of the Bayes risk in estimator selection. The Bayes risk for a decision is a linear combination of the expected squared error given that the estimator is the best and the expected squared error of the estimator given that it is not the best. Thus, while the ideal selection is the estimator with minimum squared error, the Bayes estimator selection decision can be interpreted as approximating the ideal selection by choosing the estimator with minimum expected squared error.

To use this mechanism for estimator selection, the conditional density $f_{\mathbf{x}_j|\theta}(\mathbf{x}_j|\vartheta)$, referred to as the estimator performance prior; the prior $f_\theta(\vartheta)$; the normalization matrix N ; and the weighting factors κ and τ must first be determined. Once these have been determined, the selection of a best estimator, in a minimum expected-squared-error sense, is straightforward using (18) and (22).

C. Optimality

The squared-error cost function of (20) specifies that Bayes estimator selection chooses the estimator with minimum squared error. The optimal estimator selection is defined as selecting the decision rule corresponding to the estimate that has minimum squared error. It is not possible to perfectly choose the optimal selections; however, optimal estimator

TABLE I
WIND AND RAIN ESTIMATOR SUMMARY

Estimator	$\mathcal{M}_r(\vartheta)$	ζ^2	$\hat{\vartheta}$
WO	$\mathcal{M}(\mathbf{w})$	$(1 + K_{pc}^2) [\mathcal{M}(\mathbf{w})^2 K_{pm}^2] + \mathcal{M}(\mathbf{w})^2 K_{pc}^2$	$\hat{\mathbf{w}}$
SWR	$\mathcal{M}(\mathbf{w})\alpha_r(r, p) + \sigma_e(r, p)$	$(1 + K_{pc}^2) [\alpha_r(r)^2 \mathcal{M}(\mathbf{w})^2 K_{pm}^2 + \sigma_e(r)^2 K_{pe}^2] + \mathcal{M}_r(\vartheta)^2 K_{pc}^2$	$\hat{\mathbf{w}}, \hat{r}$
RO	$\sigma_e(r, p)$	$(1 + K_{pc}^2) [\sigma_e(r)^2 K_{pe}^2] + \sigma_e(r)^2 K_{pe}^2$	\hat{r}

selection performance can be approached by maximizing the probability of selecting the optimal decision rule.

The conditional probability of selecting the optimal decision rule given the true conditions can be expressed as

$$p(\phi_{opt}|\vartheta) = \sum_{j=1}^M p(\phi_j | C(\vartheta, \mathbf{x}_j) < C(\vartheta, \mathbf{x}_i) \forall i \neq j) \quad (23)$$

which can be used to calculate the overall probability of selecting the optimal decision $p(\phi_{opt})$ using the Bayes rule

$$p(\phi_{opt}) = \int p(\phi_{opt}|\vartheta) f_{\theta}(\vartheta) d\vartheta. \quad (24)$$

For Bayes estimator selection with the specified loss function, the weighting parameters τ and κ can be viewed as parameters which allow for tuning to achieve optimal performance. As τ and κ are related, the optimal operating point can be determined by solving

$$\frac{\partial p(\phi_{opt})}{\partial \kappa} = 0 \quad (25)$$

for κ . Although in general there is no closed form for $p(\phi_{opt})$, it can be approximated reliably via Monte Carlo simulation.

D. Limitations and Advantages

There are several advantages of adopting the Bayes estimator selection technique. For instance, there is no requirement on how the estimators are formed. For example, the estimates can be maximum *a posteriori* estimates, maximum likelihood estimates, or a combination of the two. This advantage allows estimates to be formed with or without priors. Furthermore, the technique can be adapted to include multiple priors based on factors not normally included in the estimation process. For example, in the case of wind and rain estimation, such priors could include regional or topographic features, wind models for hurricanes or other phenomena, latitude-dependent rain models, or other models which may be appropriate to a local area. Considering such priors is beyond the scope of this paper.

A principle advantage of the method is that the dimensionality of the estimators need not be identical. Thus, an estimator can estimate only a subset of parameters involved. This can reduce variability and sensitivity to particularly noisy or dominant components. This allows Bayes estimator selection to produce overall performance improvements as some component sensitivities are reduced by selecting estimators that minimize such sensitivities. Finally, in addition to selecting estimates that have lower overall error, the estimator selections can be viewed as a type of contamination or impact flag. Such a flag can indicate where a particular estimate component may be particularly noisy or prone to error.

TABLE II
NORMALIZATION MATRIX VALUES

Parameter	Maximum Value	Normalization Coefficient
Wind Speed	50 m/s	1/50 ²
Wind Direction	360 deg	0
Rain Rate	250 km-mm/hr	1/250 ²

Despite these advantages, there are some limitations. As with any Bayesian technique, the overall performance is strongly dependent on the prior density. If the prior densities needed to compute the posterior expected loss are poorly defined or unknown, there may be little benefit in adopting a Bayes estimator selection structure. However, in many cases, an approximate prior is appropriate and can lead to overall performance improvement despite uncertainty in the prior. Another limitation is that the computation of the posterior expected loss can be computationally intense, particularly when it must be computed for every estimator. Fortunately, the posterior expected loss can be tabulated for many cases, and the real-time computation can be significantly reduced by approximating the Bayes risk calculation with a lookup table.

V. APPLICATION TO QUIKSCAT

A. Normalization

To apply Bayes estimator selection to QuikSCAT wind and rain estimation, a normalization matrix N is required that defines the relative importance of wind and rain error. It is important that the normalization matrix be selected so that the wind and the rain error are comparable. A useful normalization matrix has the components shown in Tables I and II. Note that the direction error is neglected. For QuikSCAT wind and rain retrieval, there are multiple possible wind and rain vectors, called “ambiguities,” for both WO and SWR estimations. Typically, the wind speed and rain rates of the ambiguities are comparable, but the wind direction estimates are separated by 90° or 180°. Choosing a single ambiguity for each estimator is termed “ambiguity selection” and is typically performed independent of wind and rain estimation [16], although, in some cases, model-based retrieval can minimize the need for ambiguity selection [17]. Because of the ambiguous nature of wind estimation, we ignore the ambiguity selection step and choose a normalization of 0 for wind direction.

To account for the different wind speed and rain rate scales, we use the normalized-squared-error cost function defined in (21). The normalization matrix N is selected to weight the components according to the selection criteria. For wind and rain estimation, we select values for the matrix N to weight each component according to the maximum retrievable value. Thus, the normalization factors for wind speed and rain rate in Table II are the reciprocal of the maximum retrievable value squared.

Additionally, although directional ambiguities exist [18] in both WO and SWR estimates, the estimated wind speeds and rain rates for each estimator are typically quite close in magnitude for all ambiguities. In this paper, we simplify the ambiguity selection process by always choosing the ambiguity which is nearest to the NCEP model winds. Although always choosing the ambiguity nearest NCEP winds simplifies the ambiguity selection procedure, the low resolution of NCEP winds can lead to selection errors. NCEP wind estimates are produced at a lower temporal and spatial resolution than QuikSCAT wind products, so there can be significant local variations. Additionally, NCEP wind models do not account for rain events or coastal topography, which can have small-scale but significant influences on wind directions. However, to simplify the estimator selection problem and minimize directional bias from the estimators or NCEP winds, we choose to ignore the estimated direction in the estimator selection error function. Thus, the normalization factor for wind direction in Table II is set to 0. Similarly, to calculate the squared error (21) for estimators that do not estimate all parameters, the parameters that are not estimated are treated as 0.

B. Wind–Rain Prior

The wind–rain prior $f_{\theta}(\vartheta)$ used in (22) requires knowledge of the distribution of wind and rain. Since wind and rain interactions are not entirely understood, we choose to approximate the true wind–rain distribution using a combination of NCEP wind estimates and measured rain data from the Tropical Rain Measuring Mission Precipitation Radar (TRMM PR) [19]. Using data from one year of QuikSCAT and TRMM PR colocated measurements, we form an empiric prior by binning numeric wind estimates and measured rain rates. Limitations of this prior are that it is susceptible to the bias of the NCEP-predicted wind and the effects of the limited sample size of the data.

To mitigate bias due to the sample size of the data, we assume that, on a global scale, the wind direction distribution is uniform. Although this neglects orographic effects and trade winds, a global prior is appropriate for wind estimation on a global scale.

After smoothing the prior, we adjust it to compensate for bias from NCEP winds in the wind model. Although there are several treatments to adjust and tune the winds, we limit our adjustments to compensating for the fact that NCEP winds poorly represent the highest wind speed cases. Since NCEP winds are predicted at a lower resolution than QuikSCAT products, the highest wind speeds are consistently averaged out of the NCEP product since they are typically not sustained over large areas. This is in addition to a fixed maximum model wind speed used in NCEP winds. In essence, the wind speed distribution of NCEP winds is truncated above a moderate wind speed.

The distribution of wind speed has Weibull characteristics [20]; therefore, to extend the wind–rain prior to high wind speeds, we perform a nonlinear least squares fit of a Weibull distribution to the empiric speed distribution for each rain rate bin and wind direction. The resulting wind–rain distribution shown in Fig. 3 is nearly identical to the empiric distribution and includes a nonzero probability of high wind speeds. The

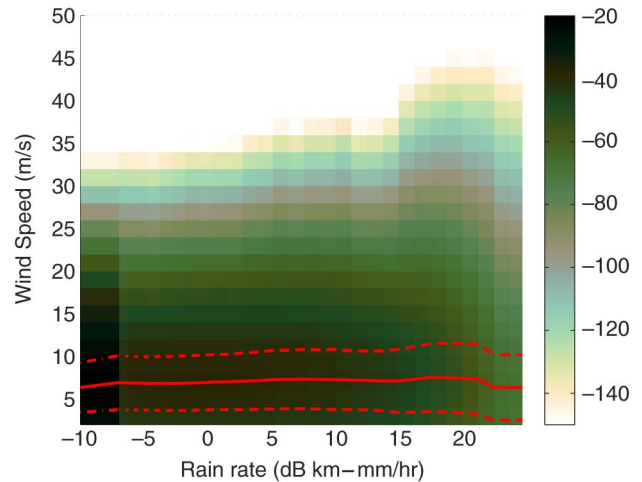


Fig. 3. Wind–rain prior distribution for a single wind direction. The color scale represents the value of $f_{\theta}(\vartheta)$ in decibels for a specific wind speed and rain rate. The solid line corresponds to the mean wind speed of the prior, and the dashed lines mark one standard deviation above and below the mean. Note that the standard deviation increases with rain rate. The zero rain rate prior is plotted as well and corresponds to the lowest rain rate in the figure. Note that the WO prior is significantly greater than the nonzero rain priors.

simple distribution fitting technique used here is adequate for our needs, although other fitting techniques exist [20]–[22].

C. Estimator Performance Prior

The estimator performance prior $f_{\mathbf{x}|\theta}(\mathbf{x}_j|\vartheta)$ reflects the probability of an estimator having minimum squared error given the true conditions. As there is no closed form for the probability densities of each estimator, there is no closed form for the estimator performance prior. This limitation can be overcome in one of several ways. Here, we adopt a simple method based on Monte Carlo simulation.

For each wind and rain vector, we generate multiple simulated backscatter observations. These are inputs to the WO, SWR, and RO estimators. The estimator performance prior is calculated from the estimates as the percentage of the realizations for which a given estimator has lower normalized squared error than the other estimators according to (21).

Fig. 4 shows the Monte Carlo simulated estimator performance prior for a fixed wind direction and cross-track location. The SWR estimator is best for most wind and rain vectors. As expected, however, when the wind speed is low and the rain is high, the RO estimator is superior. Likewise, when the wind is high and the rain is low, the WO estimator has better performance. As expected, there are relatively few cases where the RO estimator is superior.

D. Optimality

Finding the optimum operating point consists of finding the value for κ that maximizes the probability of correct estimator selection $p(\phi_{opt})$. Lacking a closed form for the probability densities of the individual estimators, we turn to Monte Carlo simulation to approximate $p(\phi_j|C(\vartheta, \mathbf{x}_j) < C(\vartheta, \mathbf{x}_i) \forall i \neq j)$ which can be used to calculate $p(\phi_{opt})$.

The Monte Carlo simulation consists of generating 1000 independent backscatter realizations for each true wind and rain

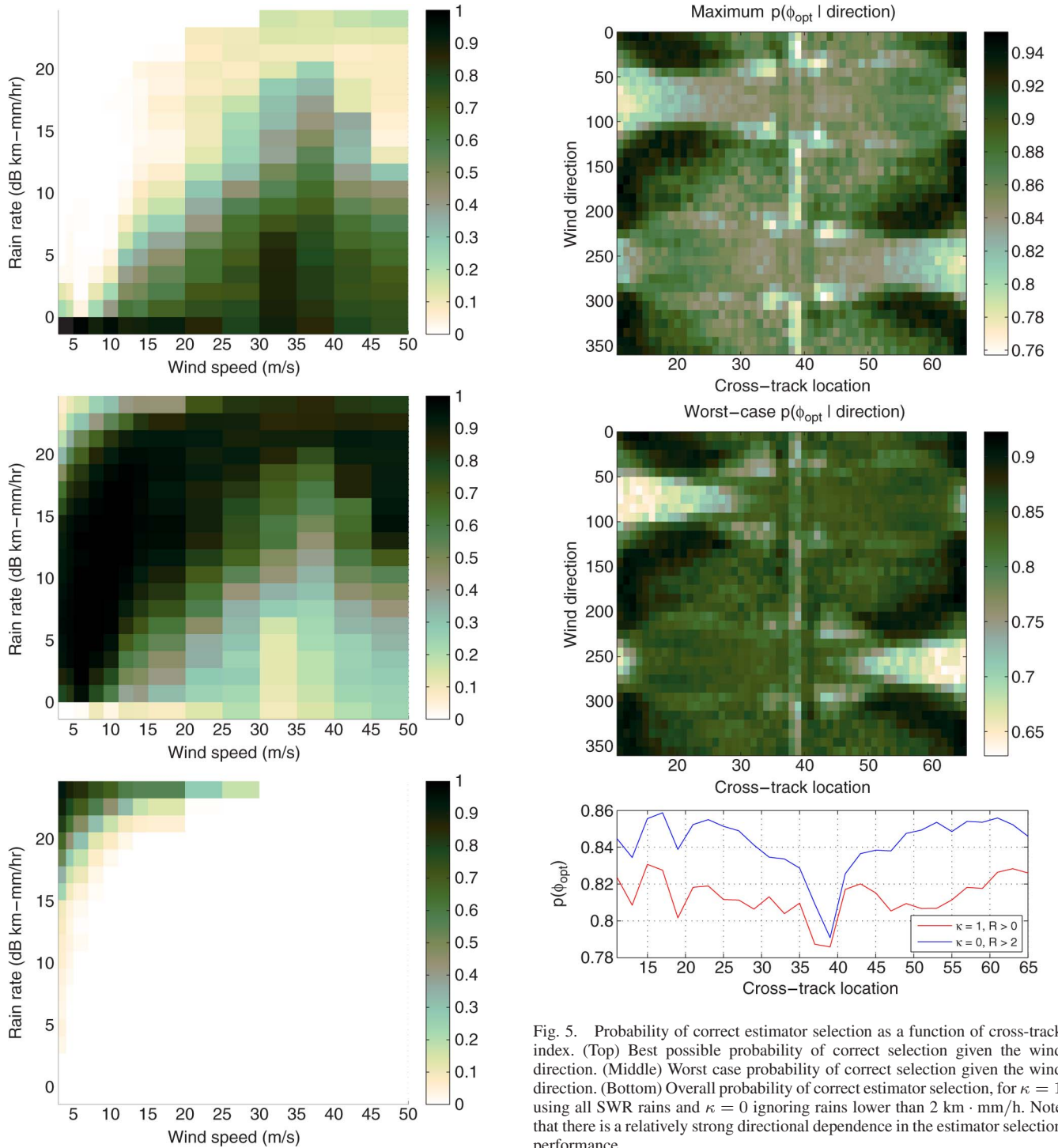


Fig. 4. Monte Carlo simulated probability of each estimator having minimum squared error. Each image represents the percentage of the time that a given estimator was selected for the underlying simulated wind and rain conditions. (Top) WO. (Middle) SWR. (Bottom) RO.

vector. Bayes estimator selection is performed for candidate values of κ on the resulting WO, SWR, and RO estimates. The optimal value for κ is that which maximizes $p(\phi_{opt})$. The probability of correct estimator selection is shown as a function of κ in Fig. 5.

An interesting feature of Fig. 5 is that wind direction can influence the probability of correct selection even though the direction error is ignored during estimator selection. Cross-track

Fig. 5. Probability of correct estimator selection as a function of cross-track index. (Top) Best possible probability of correct selection given the wind direction. (Middle) Worst case probability of correct selection given the wind direction. (Bottom) Overall probability of correct estimator selection, for $\kappa = 1$ using all SWR rains and $\kappa = 0$ ignoring rains lower than 2 km · mm/h. Note that there is a relatively strong directional dependence in the estimator selection performance.

winds (90° and 270°), a known signature of rain contamination, have the lowest probability of correct selections. Near the nadir track (cells 38 and 39), the probability of correct selection is particularly low for along-track winds. This is not surprising as the observation geometry for along-track winds is particularly poor along the nadir track, so wind and rain estimates are noisier than other swath locations. With noisier estimates, it is more difficult to choose the estimate with minimum squared error consistently, so the probability of correct selection drops.

Also shown in Fig. 5 is the probability of correct selection corresponding to the worst case value of κ . The worst case

performance has similar characteristics to the optimal performance but is 16% lower for the worst cases. However, for most cases, the difference between optimal and worst case performance is 2% to 4% which indicates that estimator selection is not particularly sensitive to the selected value for κ . The minimum value of the worst case estimator selection performance is 63%, which is a lower bound on the average estimator selection performance. This is not a very high lower bound, but it is almost twice the probability of correct selection compared to a simple ternary randomized rule which would choose correctly 33% of the time. The worst case estimator selection performance occurs for cross-track winds for certain observation geometries. Wind and rain estimation is particularly difficult for these conditions as the wind and rain signals are not orthogonal [4]. The worst case estimator selection performance for other wind directions and observation geometries is significantly better, thus allowing the average probability of correct estimator selection to be above 80% for most cases.

The optimum value for κ has an interesting interpretation. When $\kappa = 1$, the best estimator selection is given by minimizing the error associated with the correct estimator. When $\kappa = 0$, the optimum selection can be interpreted as choosing the estimator that minimizes the error associated with using an incorrect estimator. This interpretation leads to a simple explanation for the optimum values of κ . When estimator noise is high, it is best to minimize errors associated with incorrect selections by setting κ close to 0. When estimator noise is low, it is best to minimize the error associated with the correct selection, so κ is close to 1.

The optimum value for κ based on Fig. 5 is 1 for all cross-track locations. Based on the aforementioned interpretation, this implies that estimator noise is high. This noise may be largely attributed to the SWR estimator which has high noise levels for low rain rates. Much of this noise can be removed by discarding any SWR solution with a rain rate below a threshold. Setting a threshold at 2 km · mm/h increases $p(\phi_{opt})$ by up to 4% overall and changes the optimal κ value to 0, implying that estimator noise levels for these cases are lower. Since the impact of such low rains on the WO estimates is quite small and SWR estimates are particularly noisy for low rains, thresholding low rain rates for SWR reduces estimator noise without significantly increasing the overall estimate error.

VI. RESULTS

We evaluate the performance of Bayes estimator selection in several ways. First, we consider an illustrative case study. Then, we evaluate the overall estimator selection skill and consider how close Bayes estimator selection approaches the optimal decision rule. Finally, we compare overall wind and rain performance by comparing Bayes estimator selection performance to that of the individual estimators.

A. Case Study

To illustrate the functionality of Bayes estimator selection on real data, we consider a case study from QuikSCAT rev 2882 on January 7, 2000.

The WO estimates are shown in the upper left image of Fig. 6. Comparing the WO estimates to the TRMM PR-measured rain rates (lower left image in the same figures) illustrates the effects of rain contamination. Rain events cause an increase in the wind speed estimates as large as 10 to 20 m/s. Note that, for this case, the true underlying wind field varies between 5 and 10 m/s. In locations where TRMM PR did not measure rain, the WO estimates are between 5 and 10 m/s due to the underlying wind field.

The corresponding RO estimates are shown in the middle left image of Fig. 6. Comparing the RO estimates to the TRMM PR measurements shows that the RO estimates are spatially correlated with the TRMM PR-measured rain rates. As expected, the RO estimates where TRMM PR measured no rain are biased high.

The SWR estimates overcome many of the problems associated with the WO and RO estimators but also have limitations. The SWR wind estimates are shown in the upper middle image of Fig. 6, and the SWR rain estimates are shown in the center image. The SWR wind estimates are visually noisier than the WO estimates, particularly in areas where there is no rain. The opposite is true of the SWR rain estimates. The SWR rain estimates correspond well with the TRMM PR measured rain estimates for moderate rain rates; however, for the most extreme rain events, there is no SWR rain estimate. In essence, this corresponds to the case where the rain backscatter so completely dominates the wind backscatter that a wind estimate is not possible. For rain-free and low-rain cases, the SWR rain estimates are quite noisy, which helps illustrate why it is reasonable to discard the lowest SWR rain estimates as discussed in Section V-D.

The wind–rain estimates produced using the Bayes estimator selection, in effect, attempt to use the best features of each estimator. The Bayes-selected wind estimates are shown in the upper right image of Fig. 6, the Bayes-selected rain rates are shown in the middle right image, and the Bayes estimator selections are shown in the lower right image. Note the visually improved wind and rain performance. Rain estimates match the TRMM PR measured rain rates quite well. The wind field is visually smoother in nonraining conditions, and the high wind speeds due to rain contamination are no longer apparent. For reference, the ideal estimator selections, the selections which minimize the normalized squared error between the estimate and the true values, are shown in the bottom image. Note that the Bayes estimator selections and the ideal selections are noisy but are often identical.

Although there is significant improvement gained by using the Bayes-selected estimates, some drawbacks remain. For the highest rain rates, the RO estimator is selected, and consequently, there is no wind estimate. Similarly, the wind estimates corresponding to moderately high rain rates where the SWR is selected have wind estimates which underestimate the true wind speed. These wind underestimates correspond to cases in which the rain attenuation of the wind signal is significant enough to lower the wind estimates but not quite large enough to make wind estimation impossible.

The visual correlation between the Bayes-selected rain estimates and the TRMM PR measurements is good but gives no

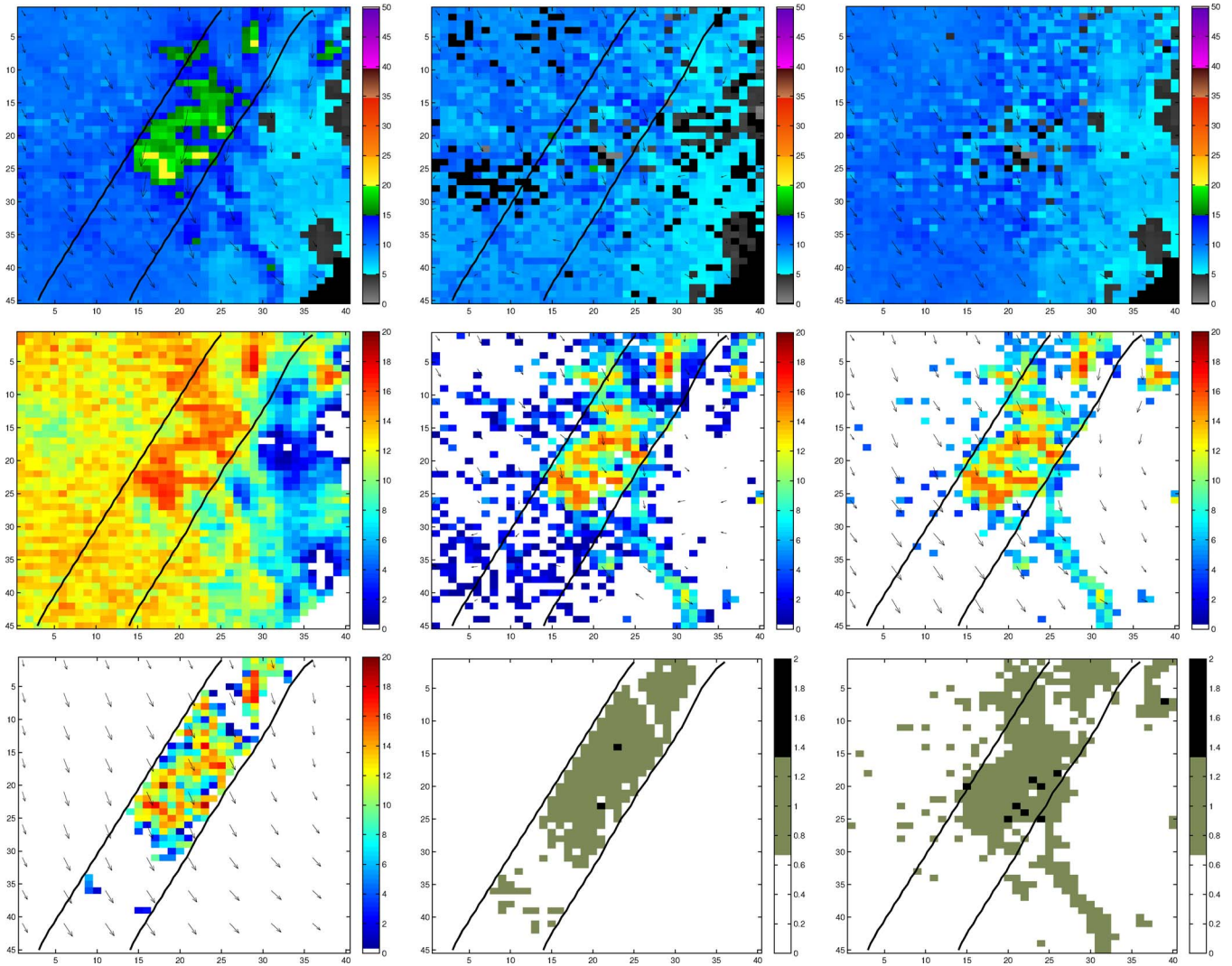


Fig. 6. 25-km-resolution estimator results and Bayes estimator selection for a particular case (QuikSCAT rev 2882 on January 7, 2000). The top row shows wind speed (in meters per second) estimates with down-sampled direction vectors overlaid. From left to right: WO, SWR, and Bayes-selected wind. The middle row shows rain estimates ($\text{dB} \cdot \text{km} \cdot \text{mm/h}$) with relevant direction vectors overlaid. From left to right: RO, SWR, and Bayes-selected rain. For comparison, the bottom row shows the TRMM PR measured rain ($\text{dB} \cdot \text{km} \cdot \text{mm/h}$) with the (bottom left) NCEP wind vector field overlaid, the (bottom center) ideal estimator selections, and the (bottom right) Bayes estimator selections. For estimator selections, 0 corresponds to a WO selection, 1 to an SWR, and 2 to a RO selection. In each image, the selected wind vectors are those closest to the NCEP wind field. Note that the Bayes-selected estimates have visually less noise than the SWR estimates and have smooth wind fields in nonraining cases.

information about the pointwise accuracy of the estimates. To evaluate the pointwise performance of the estimator selection, the selected rain estimates and the TRMM PR measurements are shown in the scatter plots in Fig. 7. The correlation for QuikSCAT rain estimates and TRMM PR rain measurements above $5 \text{ dB} \cdot \text{km} \cdot \text{mm/h}$ is 0.76.

B. Overall Decision Performance

To evaluate the performance of Bayes estimator selection, a data set of QuikSCAT and TRMM PR-colocated observations from September 1999 to December 2005 is used in the remainder of this paper. This evaluation data set contains over 1.2 million wind vector cells (WVCs) where QuikSCAT and TRMM PR made nearly simultaneous observations, within 10 min, in the vicinity of a rain event. Although some wind and rain cases are not found in the data set, the data set gives a good idea of the general performance.

The success of the Bayes estimator selection technique can be summarized most succinctly by determining how close to optimal selection the technique performs on real data. As discussed previously, optimal estimator selection consists of selecting the estimate which has minimum squared error. The percentage of time that the minimum-squared-error estimate is selected gives a measure of the algorithm performance.

To demonstrate actual estimator selection performance, Fig. 8 shows the percentage of time that the Bayes estimator selections chose the optimal estimate as a function of NCEP wind speed and TRMM PR rain rate.

Noticeably, there are some wind and rain combinations, low wind speeds, and nonzero rain rates for which estimator selection does not work well. Fortunately, the cases with poor selection accuracy are relatively rare. Furthermore, although the optimal estimator is not always selected for many of these cases, the difference between the WO and SWR estimators is small. For example, during low winds and nonzero rain, the

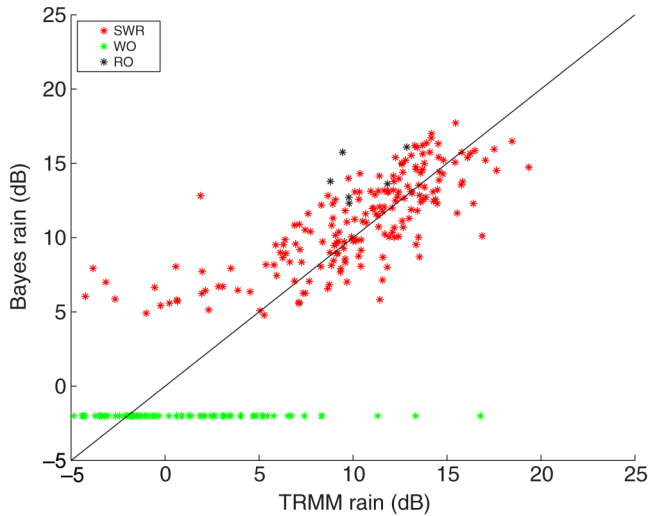


Fig. 7. 25-km-resolution Bayes-selected rain estimates as a function of TRMM PR-measured rain rates. Both axes show rain rate in dB · km · mm/h. The red points correspond to SWR rain estimates, the black to RO estimates, and the green show TRMM PR rain rates corresponding to WO selections. The one-to-one line is shown for comparison. Note that, above a TRMM rain rate of 5 dB, the correlation between QuikSCAT estimates and TRMM measurements is clear.

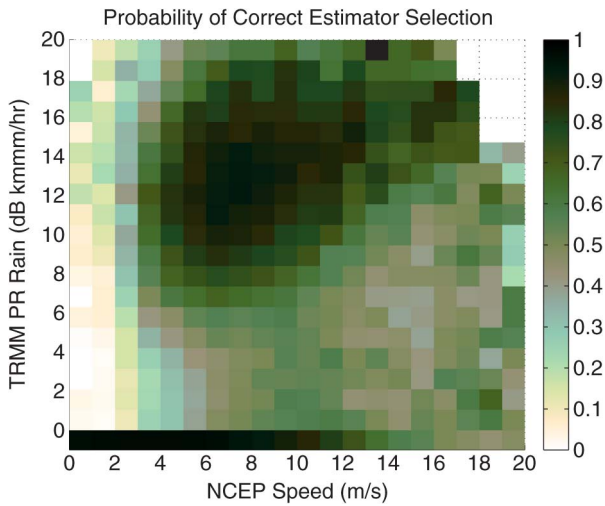


Fig. 8. Probability of correct estimator selection as a function of NCEP wind speed and TRMM PR rain rate. Nonraining performance is shown as rain rates below 0 dB · km · mm/h. Data are missing for some wind and rain vectors which did not occur in the data set. Note that, although there is poor selection performance for some cases (low speed and nonzero rain in particular), the probability of correct selection is high for the most common winds and rains.

probability of optimal selection is low as the WO estimate is typically selected when the SWR is often the best. For low rains, the effects of rain are small, so a choice of the WO estimate when the SWR is better only causes a small change in the overall error. This is also true for moderate to high speeds when the rain is low.

The probability of wind and rain conditions occurring, given that the probability of correct estimator selection is in a certain range, is shown in Table III. As shown in the table, wind and rain conditions for which the estimator selection performance is poor are relatively rare.

As expected, the Bayes estimator selections are the best for conditions with wind speeds which are close to the mean of

TABLE III
PROBABILITY OF WIND AND RAIN VECTOR GIVEN THE ESTIMATOR SELECTION PERFORMANCE

Correct selection range	Wind and rain vector
0 - 25%	0.8%
25% - 50%	4.4%
50% - 75%	10.6%
75% - 100%	84.2%

the wind and rain prior used to calculate the Bayes risk. This implies that the estimator selection algorithm is sensitive to the wind and rain prior. This sensitivity can be reduced by using a prior selection technique to be discussed in a following paper.

An evaluation of the effectiveness of Bayes estimator selection looks at the performance of the Bayes-selected estimates compared to the performance of the individual estimators as well as the optimally selected estimates. To make such a comparison, we first define rain impact. Rain impact is a condition in which the rain has a large enough impact on the WO estimate that the SWR or RO estimate has minimum squared error. This is equivalent to the optimal estimator selection being SWR or RO. With this definition for rain impact, the optimal estimator selections are the WO estimator when there is no rain impact and the SWR estimator when there is rain impact. Fig. 9 compares the wind estimate effects of rain impact using the WO estimates, the Bayes-selected estimates, and the SWR estimates.

Without Bayes estimator selection or something equivalent, only a single estimator is used. There are two choices, use the WO estimator all the time and discard rain-impacted winds, or reduce rain impact by using the SWR estimator all the time. Choosing the SWR estimator can reduce the impact of rain but suffers degraded performance when there is no rain. Bayes estimator selection balances both the strengths and weaknesses of the individual estimators by making an optimal choice between them. Fig. 9 shows that choosing the first option has good wind performance in conditions with no rain impact, but there is strong bias and high variability in rain impact conditions. On the other hand, Fig. 9 shows that using the SWR estimates gives good wind performance in rain-impact conditions but has biased performance in conditions without rain. Bayes estimator selection attempts to obtain optimal performance, using the WO estimates when there is no rain impact and the SWR estimates when there is rain impact.

To evaluate the accuracy of the rain estimates, Fig. 10 shows a scatter density plot of the TRMM PR-measured rain rates and the Bayes-selected QuikSCAT rain rate estimates. We note that the QuikSCAT rain rates are relatively unbiased compared to the TRMM PR observations, although there is significant variability in the rain estimates. A more complete discussion of SWR rain accuracy can be found in [5].

C. IMUDH Comparison

The impact-based multidimensional histogram (IMUDH) rain flag is a modified version of the multidimensional histogram (MUDH) rain flag [8] that is included with standard QuikSCAT 25-km wind estimates [12]. IMUDH is designed

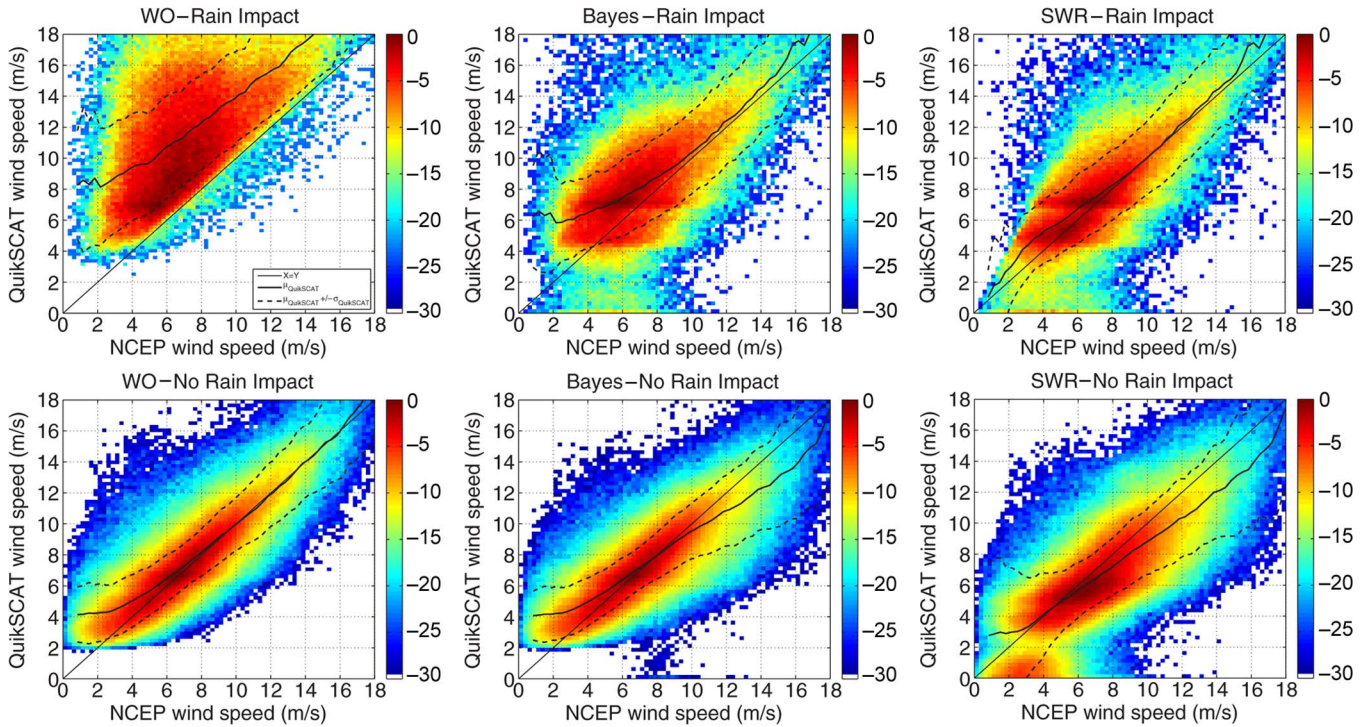


Fig. 9. Scatter densities (in decibels) for NCEP and QuikSCAT wind estimates for conditions (top row) with a rain impact, i.e., the optimal selection is the SWR estimator, and (bottom row) without a rain impact, for which the optimal selection is the WO estimator. From left to right, the columns show the WO estimates, the Bayes-selected estimates, and the SWR estimates. Each figure also includes the mean of the QuikSCAT estimates (solid black line) plus and minus one standard deviation (dashed black lines). Note that the Bayes-selected estimates have significantly reduced the wind bias in rain impact cases for all but the lowest wind speeds and have no bias in cases with no rain impact cases. Ideally, the Bayes estimates have the performance of the WO estimator in conditions with no rain impact and the same performance as the SWR in conditions with rain impact. The differences observed are due to nonoptimal estimator selection.

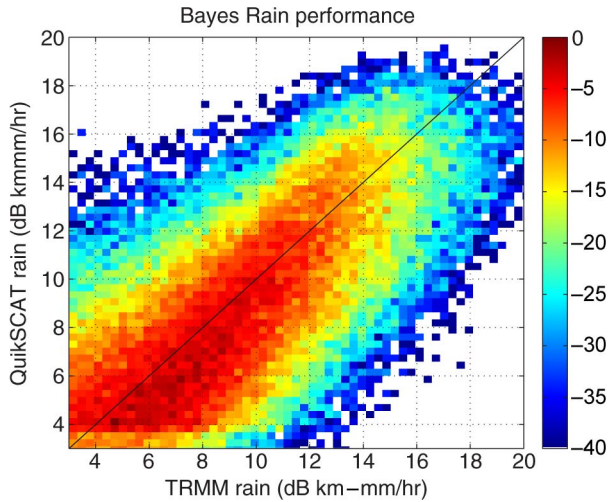


Fig. 10. Normalized scatter density in decibels of Bayes-selected rain estimates and TRMM PR rain measurements.

to indicate the likelihood of rain impact on a given wind estimate. For the IMUDH rain flag, rain impact is defined as the wind estimate being perturbed by rain from the true wind by more than 2 m/s. Although this definition is different from the definition of rain impact used previously in this paper, the IMUDH rain flag is a useful comparison tool.

An evaluation of the effectiveness of Bayes estimator selection at reducing the effects of rain can be performed using the IMUDH flag. Such a comparison requires knowledge of the true conditions. Since true wind data are unavailable, the estimate error for the WO, SWR, and Bayes-selected wind estimates

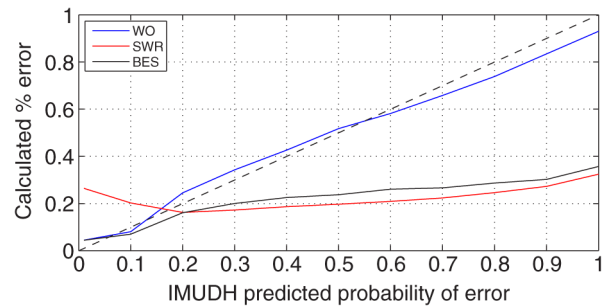


Fig. 11. Probability of the wind estimates having error greater than 3.92 m/s, as a function of the IMUDH rain flag value. The IMUDH flag correctly predicts the number of perturbed WO estimates, whereas the Bayes estimator selections and SWR estimates are perturbed by rain far less often than predicted by the IMUDH rain flag. The dashed line is a one-to-one line shown for comparison.

is calculated using NCEP model wind speeds, which have additional uncertainty. The additional uncertainty in NCEP wind speeds increases the probability that the wind estimates have error greater than 2 m/s, the original threshold for wind perturbation used in the IMUDH rain flag [12].

An appropriate IMUDH error threshold for use with NCEP model winds can be obtained. The threshold is chosen by minimizing the difference between the probability that the WO estimate error is greater than the threshold and the probability predicted by the IMUDH rain flag. For the comparison data in this paper, the threshold that minimizes the difference between WO estimate error and the IMUDH flag is 3.92 m/s. This value allows us to use the IMUDH rain flag with NCEP winds as validation wind data. Fig. 11 shows the probability of the WO,

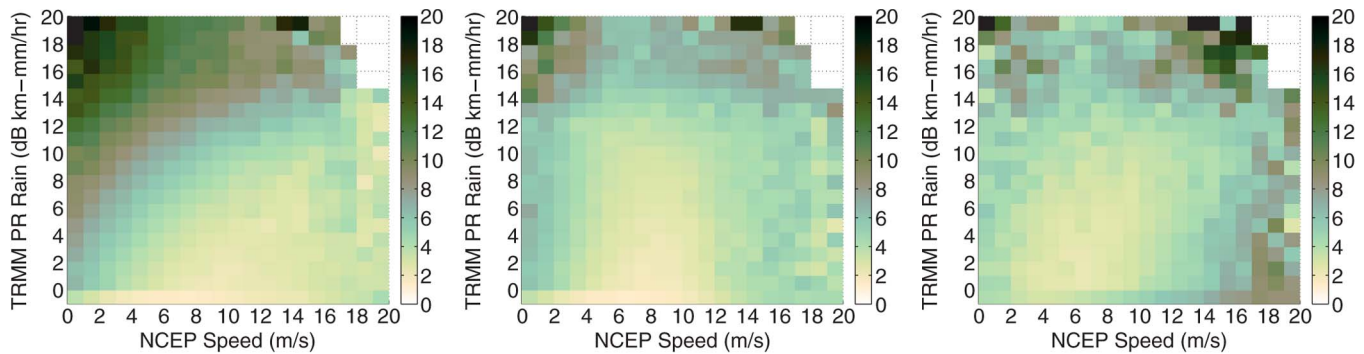


Fig. 12. Wind speed rms error (in meters per second) between the QuikSCAT estimated wind speed and the NCEP model wind speed for the (left) WO, (center) BES, and (right) SWR wind speed estimates. Note that, although the BES rmse is slightly higher than the WO rmse for high wind and low rain, it is much lower than the WO rmse for low to moderate winds with nonzero rain rates.

SWR, and Bayes-selected wind estimates having speed errors greater than 3.92 m/s as a function of the IMUDH rain flag.

By construction, the WO estimates in Fig. 11 correspond quite well with the IMUDH rain flag. The SWR wind estimates, however, have significantly lower rain perturbation for high IMUDH values. For low IMUDH values, the SWR speed estimates have more error than predicted by the IMUDH rain flag. The speed estimates selected using Bayes estimator selection have improved performance over both the WO and SWR estimates. For low IMUDH values, the speed estimates selected using Bayes estimator selection are perturbed similarly or less often than the WO estimates, and for high IMUDH values the selected speed estimates are perturbed far less often than the WO estimates and only slightly more than the SWR speed estimates.

Thus, the Bayes estimator selection (BES) performance as a function of the IMUDH flag agrees with the rain-impact performance shown in Fig. 9. In both cases, using the Bayes-selected estimates results in improved performance over the individual WO or SWR estimates for situations with and without rain impact. To summarize, Bayes estimator selection, as applied to QuikSCAT wind and rain retrieval, can reduce the effects of rain impact, thereby improving wind estimates by reducing rain contamination. It also produces estimates of the rain for rain-impacted situations.

D. Wind Speed Accuracy

A final simple measure of Bayes estimator selection performance is the wind speed rms error. Since QuikSCAT was intended to measure near-surface wind vectors, a measure of the utility of the Bayes estimator selection technique is to quantify the improvement to this specific function. As noted previously, although NCEP wind data are subject to a number of limitations, on a large scale, it provides a useful comparison data set for this analysis.

The wind speed rms error is calculated for the WO, SWR, and Bayes estimator selected wind estimates as a function of NCEP wind speed and TRMM PR measured rain rate for the data set described in Section VI-B. Fig. 12 shows the calculated rms error levels for the evaluation data set. As might be expected, the WO estimates have lower wind speed rms error for conditions with low rain. The SWR wind speed rms

error is lower than the WO for moderate to high rain rates but is higher for low rain rates with high wind speeds. However, BES provides overall better performance since it is designed to choose the WO estimates for nonraining cases and the SWR estimates during rain events.

As indicated by the Bayes-selected wind speed rms error in Fig. 12, the rms error is lower than the WO estimates for low to moderate winds during rain events but is slightly higher than the WO rms error for high wind speeds with low rain rates. However, for moderate winds and low to moderate rains, the Bayes-selected wind speed rms error is lower than either the WO and SWR rms error. Thus, as hoped, the Bayes estimator selection technique balances the strengths of the WO and SWR wind estimates, producing wind estimates and rain estimates which can have lower rms error than either the WO or SWR estimates individually.

VII. CONCLUSION

Bayes estimator selection is a unique way of addressing QuikSCAT wind and rain estimation. Rather than relying solely on one type of estimator, we can use Bayes estimator selection to reduce the effects of rain impact without discarding information. This improves the overall quality and reliability of the wind and rain estimates. Furthermore, Bayes estimator selection is a highly flexible and robust technique which can be adapted to a variety of problems regardless of estimator type or dimension. Although the technique does not always make the optimal selections, it does so a large majority of the time. This reliability makes Bayes estimator selection a valuable tool to increase the functionality of QuikSCAT data products as well as those from other scatterometers such as ASCAT.

REFERENCES

- [1] F. M. Naderi, M. H. Freilich, and D. G. Long, "Spaceborne radar measurement of wind velocity over the ocean—An overview of the NSCAT scatterometer system," *Proc. IEEE*, vol. 76, no. 6, pp. 850–866, Jun. 1991.
- [2] D. G. Long, "High resolution wind retrieval from SeaWinds," in *Proc. IGARSS*, 2002, pp. 751–753.
- [3] D. Long, J. Luke, and W. Plant, "Ultra high resolution wind retrieval from SeaWinds," in *Proc. IGARSS*, 2003, pp. 1264–1266.
- [4] D. W. Draper and D. G. Long, "Simultaneous wind and rain retrieval using SeaWinds data," *IEEE Trans. Geosci. Remote Sens.*, vol. 42, no. 7, pp. 1411–1423, Jul. 2004.
- [5] M. P. Owen and D. G. Long, "Progress toward validation of QuikSCAT ultra-high-resolution rain rates using TRMM PR," in *Proc. IGARSS*, Jul. 2008, vol. 4, pp. 299–302.

- [6] J. R. Allen and D. G. Long, "An analysis of SeaWinds-based rain retrieval in severe weather events," *IEEE Trans. Geosci. Remote Sens.*, vol. 43, no. 12, pp. 2870–2878, Dec. 2005.
- [7] C.-Y. Chi and F. K. Li, "A comparative study of several wind estimation algorithms for spaceborne scatterometers," *IEEE Trans. Geosci. Remote Sens.*, vol. 26, no. 2, pp. 115–121, Mar. 1988.
- [8] J. N. Huddleston and B. W. Stiles, "A multidimensional histogram rain-flagging technique for SeaWinds on QuikSCAT," in *Proc. IGARSS*, Jul. 2000, vol. 3, pp. 1232–1234.
- [9] D. W. Draper and D. G. Long, "Evaluating the effect of rain on SeaWinds scatterometer measurements," *J. Geophys. Res.*, vol. 109, p. C02005, 2004.
- [10] S. N. Nielsen and D. G. Long, "A wind and rain backscatter model derived from AMSR and SeaWinds data," *IEEE Trans. Geosci. Remote Sens.*, vol. 47, no. 6, pp. 1595–1606, Jun. 2009.
- [11] B. W. Stiles and S. Yueh, "Effect of rain on Ku-band scatterometer wind measurements," *IEEE Trans. Geosci. Remote Sens.*, vol. 40, no. 9, pp. 1973–1983, Sep. 2002.
- [12] *QuikSCAT Science Data Product User's Manual*, D-18053 ed., Phys. Oceanogr. DAAC, JPL, Pasadena, CA, 2006.
- [13] D. G. Long and M. W. Spencer, "Radar backscatter measurement accuracy for a spaceborne pencil-beam wind scatterometer with transmit modulation," *IEEE Trans. Geosci. Remote Sens.*, vol. 35, no. 1, pp. 102–114, Jan. 1997.
- [14] T. E. Oliphant and D. G. Long, "Accuracy of scatterometer-derived winds using the Cramér–Rao bound," *IEEE Trans. Geosci. Remote Sens.*, vol. 37, no. 6, pp. 2642–2652, Nov. 1999.
- [15] T. K. Moon and W. C. Stirling, *Mathematical Methods and Algorithms*. Englewood Cliffs, NJ: Prentice-Hall, 2000.
- [16] S. J. Shaffer, R. S. Dunbar, S. V. Hsiao, and D. G. Long, "A median-filter-based ambiguity removal algorithm for NSCAT," *IEEE Trans. Geosci. Remote Sens.*, vol. 29, no. 1, pp. 167–174, Jan. 1991.
- [17] B. A. Williams and D. G. Long, "Estimation of hurricane winds from SeaWinds at ultrahigh resolution," *IEEE Trans. Geosci. Remote Sens.*, vol. 46, no. 10, pp. 2924–2935, Oct. 2008.
- [18] D. W. Draper and D. G. Long, "An advanced ambiguity selection algorithm for SeaWinds," *IEEE Trans. Geosci. Remote Sens.*, vol. 41, no. 3, pp. 538–547, Mar. 2003.
- [19] N. Takahashi and T. Iguchi, "Characteristics of TRMM/PR system noise and their application to the rain detection algorithm," *IEEE Trans. Geosci. Remote Sens.*, vol. 46, no. 6, pp. 1697–1704, Jun. 2008.
- [20] E. G. Pavia and J. J. O'Brien, "Weibull statistics of wind speed over the ocean," *J. Clim. Appl. Meteorol.*, vol. 25, no. 10, pp. 1324–1332, Oct. 1986.
- [21] K. Conradsen and L. B. Nielsen, "Weibull statistics for estimation of wind speed distributions," *J. Clim. Appl. Meteorol.*, vol. 23, no. 8, pp. 1173–1183, Aug. 1984.
- [22] W.-K. Pang, J. J. Forster, and M. D. Troutt, "Estimation of wind speed distribution using Markov chain Monte Carlo techniques," *J. Clim. Appl. Meteorol.*, vol. 40, no. 8, pp. 1476–1484, Aug. 2001.



MIT Lincoln Laboratory.

Michael P. Owen received the B.S. degree in electrical engineering from Brigham Young University (BYU), Provo, UT, in 2007, where he also received the Ph.D. degree in electrical engineering in September 2010 after completing his dissertation titled *Scatterometer Contamination Mitigation*.

He worked in the Microwave Earth Remote Sensing Laboratory from 2006 to 2010 on rain backscatter modeling, simultaneous wind and rain estimation, and Bayesian decision theory applications to ultrahigh resolution scatterometry. He is currently with



David G. Long (S'80–SM'98–F'08) obtained the Ph.D. degree in electrical engineering from the University of Southern California, Los Angeles, in 1989.

From 1983 to 1990, he worked for NASA's Jet Propulsion Laboratory (JPL), Pasadena, CA, where he developed advanced radar remote sensing systems. While at JPL, he was the Project Engineer on the NASA Scatterometer (NSCAT) project which flew from 1996 to 1997. He also managed the SCANSAT project, the precursor to SeaWinds which was launched in 1999 on QuikSCAT and

in 2002 on ADEOS-II. He is currently a Professor with the Electrical and Computer Engineering Department, Brigham Young University (BYU), Provo, UT, where he teaches upper division and graduate courses in communications, microwave remote sensing, radar, and signal processing and is the Director of the BYU Center for Remote Sensing. He is the principle investigator on several NASA-sponsored research projects in remote sensing and has over 390 publications in various areas, including signal processing, radar scatterometry, and synthetic aperture radar. His research interests include microwave remote sensing, radar theory, space-based sensing, estimation theory, signal processing, and mesoscale atmospheric dynamics.

Dr. Long has received the NASA Certificate of Recognition several times. He is an Associate Editor for the IEEE GEOSCIENCE AND REMOTE SENSING LETTERS.